

PAPER • OPEN ACCESS

## Real-time delivered dose assessment in carbon ion therapy of moving targets

To cite this article: C Galeone *et al* 2024 *Phys. Med. Biol.* **69** 205001

View the [article online](#) for updates and enhancements.

### You may also like

- [Opportunities and challenges of upright patient positioning in radiotherapy](#)  
Lennart Volz, James Korte, Maria Chiara Martire et al.
- [Global and local feature extraction based on convolutional neural network residual learning for MR image denoising](#)  
Meng Li, Juntong Yun, Dingxi Liu et al.
- [Modelling radiobiology](#)  
Lydia L Gardner, Shannon J Thompson, John D O'Connor et al.



## LUNA 3D The New More in SGRT



Experience safety, efficiency,  
and comfort in radiation therapy

[www.lap-laser.com](http://www.lap-laser.com)

Availability of products, features, and services may vary depending on your location.





## PAPER

## Real-time delivered dose assessment in carbon ion therapy of moving targets

## OPEN ACCESS

RECEIVED  
24 May 2024REVISED  
29 July 2024ACCEPTED FOR PUBLICATION  
19 September 2024PUBLISHED  
30 September 2024

Original content from  
this work may be used  
under the terms of the  
[Creative Commons  
Attribution 4.0 licence](#).

Any further distribution  
of this work must  
maintain attribution to  
the author(s) and the title  
of the work, journal  
citation and DOI.



C Galeone<sup>1,2,3,\*</sup> , T Steinsberger<sup>1,9</sup> , M Donetti<sup>4</sup> , M C Martire<sup>1,2</sup> , F M Milian<sup>5,6</sup> , R Sacchi<sup>3,5</sup> ,  
A Vignati<sup>3,5</sup> , L Volz<sup>1</sup> , M Durante<sup>1,7,8</sup> , S Giordanengo<sup>5</sup> and C Graeff<sup>1,2</sup>

<sup>1</sup> Biophysics, GSI Helmholtzzentrum für Schwerionenforschung, Darmstadt, Germany

<sup>2</sup> Department of Electrical Engineering and Information Technology, TU Darmstadt, Darmstadt, Germany

<sup>3</sup> Dipartimento di Fisica, Università degli Studi di Torino, Torino, Italy

<sup>4</sup> Centro Nazionale di Adroterapia Oncologica (CNAO), Pavia, Italy

<sup>5</sup> Istituto Nazionale di Fisica Nucleare, Torino, Italy

<sup>6</sup> Universidade Estadual de Santa Cruz, Ilheus, Brazil

<sup>7</sup> Institute for Condensed Matter Physics, TU Darmstadt, Darmstadt, Germany

<sup>8</sup> Dipartimento di Fisica, Università Federico II, Napoli, Italy

<sup>9</sup> Now at Brainlab, Munich, Germany.

\* Author to whom any correspondence should be addressed.

E-mail: [c.galeone@gsi.de](mailto:c.galeone@gsi.de)

**Keywords:** real-time dose calculation, particle therapy, moving targets, adaptive therapy

## Abstract

**Objective.** Real-time adaptive particle therapy is being investigated as a means to maximize the treatment delivery accuracy. To react to dosimetric errors, a system for fast and reliable verification of the agreement between planned and delivered doses is essential. This study presents a clinically feasible, real-time 4D-dose reconstruction system, synchronized with the treatment delivery and motion of the patient, which can provide the necessary feedback on the quality of the delivery.

**Approach.** A GPU-based analytical dose engine capable of millisecond dose calculation for carbon ion therapy has been developed and interfaced with the next generation of the dose delivery system (DDS) in use at Centro Nazionale di Adroterapia Oncologica (CNAO). The system receives the spot parameters and the motion information of the patient during the treatment and performs the reconstruction of the planned and delivered 4D-doses. After each iso-energy layer, the results are displayed on a graphical user interface by the end of the spill pause of the synchrotron, permitting verification against the reference dose. The framework has been verified experimentally at CNAO for a lung cancer case based on a virtual phantom 4DCT. The patient's motion was mimicked by a moving Ionization Chamber (IC) 2D-array. **Main results.** For the investigated static and 4D-optimized treatment delivery cases, real-time dose reconstruction was achieved with an average pencil beam dose calculation speed up to more than one order of magnitude smaller than the spot delivery. The reconstructed doses have been benchmarked against offline log-file based dose reconstruction with the TRiP98 treatment planning system, as well as QA measurements with the IC 2D-array, where an average gamma-index passing rate (3%/3 mm) of 99.8% and 98.3%, respectively, were achieved. **Significance.** This work provides the first real-time 4D-dose reconstruction engine for carbon ion therapy. The framework integration with the CNAO DDS paves the way for a swift transition to the clinics.

## 1. Introduction

Particle therapy offers the possibility of a highly selective dose localization compared with conventional radiotherapy, arising from both physical and biological characteristics of the energy deposition (Durante and Loeffler 2010). As a consequence, such treatments are more sensitive to uncertainties in particle's range (Lomax 2020), which may be determined by variations in the patient's anatomy (Graeff *et al* 2023), and by the target motion. The impact of such uncertainty is even bigger for heavy ions, like carbon ions, because of

the pronounced relative biological effectiveness (RBE) in the distal fall-off of the Bragg Peak. Inter-fractional anatomic changes and intra-fractional patient motions (Pakela *et al* 2022) might lead to under-dosage in the target volume and over-dosage in organs at risk. Intra-fractional motion is a major challenge in radiotherapy, in conventional but especially in particle therapy (Knopf *et al* 2022). To safely handle complex targets located in the lungs or in the abdomen, that are subject to considerable intra-fractional motion (Dhont *et al* 2018), several adaptive methods and motion mitigation strategies have been proposed and developed to minimize the interplay effect (Graeff *et al* 2023), i.e. gating (Minohara *et al* 2000, Ciocca *et al* 2016), tracking (Grözinger *et al* 2008, Riboldi *et al* 2012) and 4D optimizations using the Single Phase Uniform Dose (SPUD) approach (Graeff 2014) used for MultiPhase 4D (MP4D) delivery (Lis *et al* 2020, Steinsberger *et al* 2023).

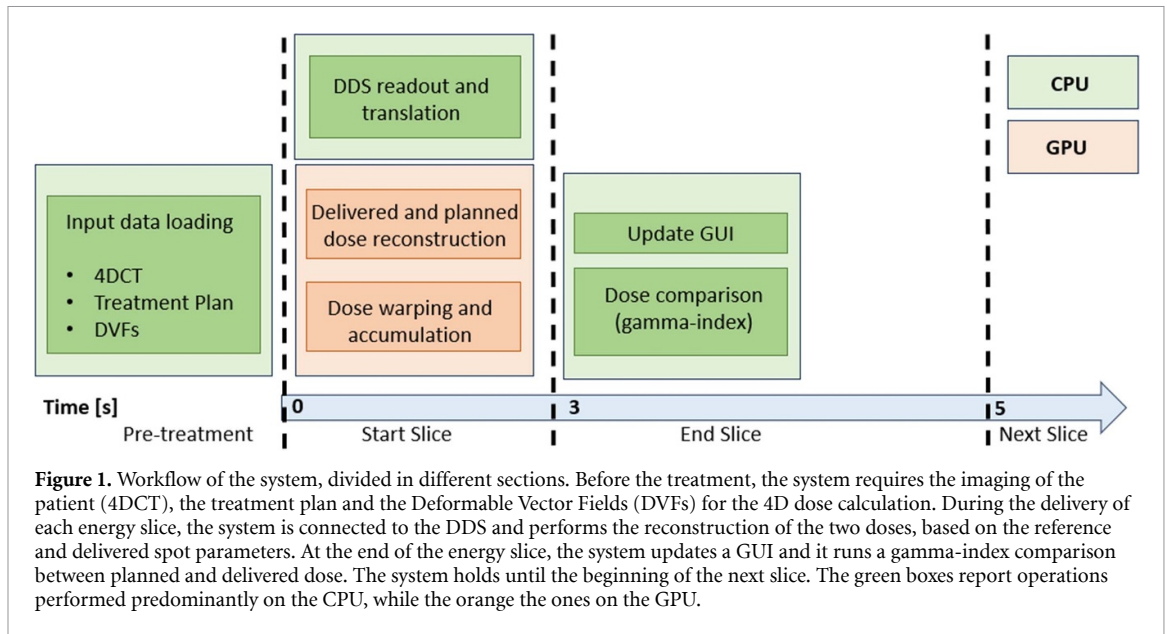
A possible approach to mitigate the effect of anatomical changes is offered by daily adaptive therapy (Albertini *et al* 2020) potentially able to cope with inter-fractional variations (Bobic *et al* 2021). One of the key aspects of daily adaptive therapy is the verification of the delivered treatment accuracy by exploiting available online measurements. Among various techniques, methods based on secondary radiation studies (positron emission tomography PET (Fiorina *et al* 2018, Parodi *et al* 2023) and prompt-gamma imaging (Krimmer *et al* 2018, Bertschi *et al* 2023)), have reached promising results followed by clinical application at some centers.

More frequently, the actual dose reconstructions are based on the log-files (Scandurra *et al* 2016, Choi *et al* 2018, Guterres Marmitt *et al* 2020), provided by the beam delivery control system containing the measured beam spot parameters: position and number of particles per spot. After the treatment, a dose calculation program reconstructs from the log-files the delivered dose distribution and compares it with the reference distribution, based on the planned spot sequence, usually by means of gamma-index analysis. This may be particularly relevant for the implementation of the motion mitigation techniques where, combining the measured spot parameters with the tracking of the patient movement, potential dose mismatches originating from the beam delivery control may be identified. Different studies have been conducted in this direction (Pfeiler *et al* 2018, Meijers *et al* 2019, Duetschler *et al* 2023). However, an integrated clinical software for time-resolved 4D delivered dose assessment is still one of the top clinical priorities, as reported by (Zhang *et al* 2023) for intra- and (Trnkova *et al* 2023) for inter-fractional adaptation. Both studies demonstrate a high interest of the particle therapy community for adaptive therapy.

According to (Trnkova *et al* 2023), daily adaptive therapy is the method of choice over a 10 years timespan, while (Zhang *et al* 2023) reports interest for real-time motion management. Real-time adaptation is considerably more challenging, as it requires real-time feedback on the treatment, and crucially, a dose engine for updating the delivered dose distribution based on the monitoring signal. A first step in this direction has been presented with the Real-time Ion Dose planning and delivery System (RIDOS) tool (Giordanengo *et al* 2019), developed within the Istituto Nazionale di Fisica Nucleare (INFN) RIDOS project. This tool proved the feasibility of an online dose calculation based on the measured spot parameters and synchronized with the delivery. A step further involves outfitting the system with the ability to provide fast feedback on the delivery quality, integrating these operations into the technical workflow of the dose delivery, thereby eliminating the need for additional tasks to be assigned to personnel for utilizing and leveraging its features.

In this work we propose a fast Forward Dose Calculation (FDC) tool, able to perform the dose reconstruction in case of moving anatomies (4D-reconstruction) on the fly. The system is designed to be integrated into the research version of the Dose Delivery System (DDS) in use at the Centro Nazionale di Adroterapia Oncologica (CNAO) (Graeff 2014) to calculate both the cumulative delivered and prescribed dose distributions, thanks to the synchronization with real-time data provided by the DDS. The aim is a system operating during the treatment to provide a prompt update on the delivery quality within the inter-spill time. The latter is characteristic of synchrotron-based facilities, which are currently the only facilities offering ion therapy (Particle Therapy Co-Operative Group 2024). However, the proposed tool can be easily integrated with other types of accelerators and it can be used for facilities using particle species different from carbon.

The core of this tool, RIDOS, was developed in previous projects to be integrated into the clinical DDS at CNAO (Russo *et al* 2015, Giordanengo *et al* 2019). The algorithm has been extended to handle 4D calculations, improve time performance, and be suitable for both the future 4D-DDS architectures in development at CNAO and GSI. As such, it is referred to as 4D-RIDOS throughout this work. A detailed description of the new hardware and software features of 4D-RIDOS will be presented together with the results of a preliminary experimental validation performed at CNAO.



## 2. Materials and methods

### 2.1. 4D-RIDOS

The 4D-RIDOS system comprises three main components: (a) an interface to the clinical DDS of CNAO, (b) the FDC which runs on GPU (developed adopting CUDA, NVIDIA's Compute Unified Device Architecture (Vingelmann and Fitzek)), with a child process on CPU to receive the spot parameters and to stream back the dose distribution to be displayed, and (c) a Graphical user interface (GUI) written in Matlab (The MathWorks Inc.). The latter handles the data transfer between all components and visualizes the planned and reconstructed dose side-by-side along with their comparison to provide an estimation of the overall treatment quality. The workflow of the 4D-RIDOS operations is detailed in the next sections.

#### 2.1.1. Workflow

The workflow of the operations performed by 4D-RIDOS is summarized in figure 1.

The FDC requires two sets of input data, one is provided offline before the start of the delivery, and the second consists of spot parameters measured by the beam monitors and acquired by the DDS. Additionally, to perform the dose calculations and 4D evaluations, a 4DCT and deformable vector fields (DVs), as well as the full treatment plan as it is intended to be delivered are required. The processing of these data runs on a standard CPU while real-time tasks are performed predominantly on the GPU.

Most of the pre-treatment input files are provided in the standard DICOM format and need to be transformed to 4D-RIDOS compliant input data. To deal with images of a moving target, a Deformable Image Registration (DIR) procedure is carried out with Plastimatch (Sharp *et al* 2010) before the delivery, aligning each CT phase with the reference one. This procedure generates a set of 3D arrays, per phase, with displacements on the three dimensions (DVs), mapping the coordinates from one CT to the corresponding coordinates of the reference CT. This step is necessary for the warping of the dose distribution from each CT to the reference one. The warping procedure was ported to CUDA and benchmarked against standard Plastimatch running on CPU, as described in section 2.3.1.

A front-end with GUI, described in section 2.1.4, manages the data transfer between the DDS and the FDC and shows the results of the computation at the end of the energy slice. Together with the spot positions and delivered particles, 4D-RIDOS was designed to receive also the detected breathing phase of each delivered spot. It traces the beam on the corresponding phase CT of the 4DCT, which is used as a surrogate of the actual patient anatomy. After the reconstruction, the planned and delivered doses are warped (see section 2.3.1), if needed, and then accumulated on the reference CT. Additionally, the GUI at the end of each energy slice runs an independent GPU gamma-index analysis to compare the two reconstructed doses.

#### 2.1.2. Hardware configuration

The system has been developed to be integrated within the research version of the CNAO DDS in order to promptly receive the measured spot parameters during the treatment deliveries. The DDS consists of commercial Field Programmable Gate Arrays (FPGAs) interfaced with the nozzle beam monitors and with



the accelerator control system to continuously measure the spot position and the number of particles delivered and to control the scanning magnets to guide the treatment according to the prescription of the treatment plan (Giordanengo *et al* 2015, Donetti *et al* 2021). Each FPGA has a dedicated task, those monitoring the spot intensity, spot position, and the currents of the scanning magnets being relevant for the communication with 4D-RIDOS. Moreover, the research version of the DDS also handles the patient's motion phase (Lis *et al* 2020, Donetti *et al* 2021, Steinsberger *et al* 2023).

The raw dose delivery data are generated every 50 ms, during beam off and at the end of each spot during beam on. They are sent via VHDCI cables to an FPGA card (NI PXIe-7720R, inside an NI PXIe-8840 crate). The FPGA bundles matching data from the four FPGAs of the DDS, and streams it via a FIFO to the crate controller. From there, the data is streamed to the laptop workstation (DELL-7760 Mobile Workstation equipped with Intel Xeon W-11855M, 62GB RAM and a NVIDIA RTX A5000 Laptop GPU), which is running 4D-RIDOS, by means of an ethernet cable and TCP/IP protocol. This hardware configuration represents a prototype of the future clinical version of the DDS at CNAO (Lis *et al* 2020). The streaming of the spot parameters between DDS and 4D-RIDOS has been designed not to interfere with the delivery (Donetti *et al* 2021).

### 2.1.3. Dose reconstruction algorithm

The real-time dose engine is based on ray-tracing and interpolation of pre-calculated Look-Up Tables (LUTs). These tasks were implemented on GPU to exploit highly parallel processing, with kernels running on thousands of threads. A further reduction in the processing time compared with the first release described in (Giordanengo *et al* 2019) was achieved by a large use of shared and local memory with coalescent memory access.

The Siddon algorithm (Siddon 1985) was used to calculate the cumulative water equivalent path length (WEPL) along the CT corresponding to each specific breathing phase, transforming the coordinates of the voxels of the medium crossed by the beam to water equivalent coordinates later employed for the dose calculation. Moreover, the program takes as input a radial cutoff in millimeters, to account for the spreading of the beam and to increase the dose accuracy. The dose computation involves the interpolation of several sets of 3D LUTs, developed to cover each possible beam energy and filled with linearly-superimposable quantities such as the absorbed dose per primary ion. The system is also able to reconstruct RBE-weighted dose via specific 3D LUTs containing linearly-superposable radiobiological quantities. However, this work focuses on absorbed doses only. For a more detailed description of the dose computation algorithm, refer to (Russo *et al* 2015, Giordanengo *et al* 2019).

The major limitation of the previous version was the selection of the voxels of interest spot by spot. In the final stage of the dose calculation, just before the interpolation of the LUTs, the system requires the position of all the voxels along the beam propagation axis within a certain radial cutoff. The original algorithm was looping over the entire CT looking for these positions, leading to severe time consumption.

The new version of the algorithm, described and characterized in this work, handles 4D deliveries and is up to 15 times faster than the original one (Giordanengo *et al* 2019). This was achieved by pre-selecting the voxels of interest per ray prior to the delivery, relying on the planned beam position at the isocenter plane. To account for position mismatches during treatment delivery, a search box area for the real beam position is created assuming a 3 mm error on X and Y is taken under consideration. Only if the delivered beam position is further mislocated than this tolerance, the algorithm switches back to the original procedure looping over the entire CT. This case is however relatively unlikely in the clinical case due to the position feedback loop based on the nozzle ionization chambers. This deviation of the delivered spot position from planned one would cause an interlock (Giordanengo *et al* 2015) which have been masked during the conducted experiments.

A further update of the algorithm involves the timing of the calculation. The dose reconstruction is triggered by three different delivery conditions: (i) the conclusion of an energy slice, (ii) the delivery of the last spot assigned to that specific phase for an energy slice, or (iii) a change in the phase during beam on. Depending on the delivery modality, the trigger works differently. In case of a static delivery, the trigger is activated by the end of each beam spill. In case of a 4D delivery, the trigger is represented by a change in the motion phase. For example, once the motion phase switches from 0 to 1, the system reconstructs the dose of all the spots of that energy slice delivered during motion phase 0. Moreover, the conclusion of the energy slice is considered a trigger to calculate the dose of the spots delivered in the last motion phase, before the energy switch.

In addition, to handle patients' motion, a dose warping section has been developed, based on Plastimatch CPU code. This procedure is carried out at the end of each calculation of each phase except for the reference one, which does not require warping.

As a further update, the interface to the DDS within the GUI has been completely overhauled and tailored to the current features of the clinical system in use at CNAO.

#### 2.1.4. Front-end software

The front-end software manages the entire 4D-RIDOS workflow, handling also the external connection to the DDS and the internal one to the FDC, triggering gamma-index calculation as well as presenting the results on a GUI.

The GUI receives the information recorded by the DDS during the delivery in real-time, including position, number of particles and motion phase per spot. It performs the readout and the translation of the raw data, prepares the input files for the dose reconstruction when a trigger occurs, as explained in the previous section, and starts the FDC to calculate planned and delivered dose distributions.

At the conclusion of the delivery of each energy slice, the two reconstructed doses are sent to the GUI for visualization. The customizable GUI shows the planned and delivered doses as well as their difference as shown in figure 3. Moreover, the GUI runs a GPU-based gamma-index analysis (Persoon et al 2011) to provide fast feedback on the accuracy of the delivery and it displays the corresponding distribution.

#### 2.1.5. Expected DVH

An additional feature is represented by 4D-RIDOS expected Dose Volume Histogram (DVH). This tool predicts the expected final dose distribution of the delivery in real-time, as follows:

$$\text{Expected Final Dose} = \text{Full Plan Dose} - \sum_i^{N_{\text{spots}}} \text{Planned Dose} + \sum_i^{N_{\text{spots}}} \text{Delivered Dose}$$

*Full plan dose* refers to the total dose distribution according to the reference treatment plan. *Planned Dose* and *Delivered Dose* are the dose distributions calculated by summing over all the spots delivered up to that point ( $N_{\text{spots}}$ ). This way the system is able to anticipate the final dose distribution, assuming a perfect delivery of the remaining spots.

The results are displayed on the GUI at the end of each energy slice, integrating also the target planned and expected DVH. This expansion of 4D-RIDOS represents a valuable solution for a possible future clinical application of the algorithm. It gives the opportunity to visualize the results in a different way, with a more intuitive understanding of the accuracy of the delivery.

## 2.2. Experimental setup

The tests have been carried out in the experimental room of CNAO providing a horizontal beamline equipped with a complete DDS modified to deliver 4D treatments.

The irradiation setup reflects a Quality Assurance (QA)-like arrangement, with an Ionization Chamber (IC) 2D-array (PTW Octavious 1500XDR, PTW, Freiburg, Germany) mounted on a programmable linear stage (PI M-414.2PD, controller PI C-884.4DC; Physik Instrumente, Karlsruhe, Germany), as represented by figure 2. The number of IC within the lateral width of the dose distribution in the Octavious 1500XDR has been maximized. The detection depth was shifted to one where the lateral area covered by the high dose region is maximal by placing polymethyl methacrylate (PMMA) plates with a total of 44 mm water equivalent thickness in front of the detector.

The linear stage acted both as a moving patient and its controller as a motion monitoring system, streaming the axis position and the phase of the movement directly to the DDS at a frequency of 1 kHz. In this simple arrangement, the tumor motion in the patient CT corresponds to a purely horizontal motion perpendicular to the beam. For a more comprehensive description of the experimental setup refer to (Steinsberger et al 2023).

The 4D-RIDOS system was integrated into the DDS as described in section 2.2.

The linear stage was programmed in order to follow a 1D regular motion. The motion trajectory matches the craniocaudal (CC) displacement of the tumor during the corresponding phase in the planning CT. The motion period was set to 3.9 s.

All the tests performed were performed with a carbon ion beam; nonetheless, 4D-RIDOS has been designed and developed to be used in CNAO also with protons.

## 2.3. Experimental verification of the algorithm

The system has been validated experimentally on a virtual 4-dimensional extended cardiac-torso (XCAT) 4DCT (Segars et al 2008, Steinsberger et al 2023). The 4DCT was created as illustrated in a previous

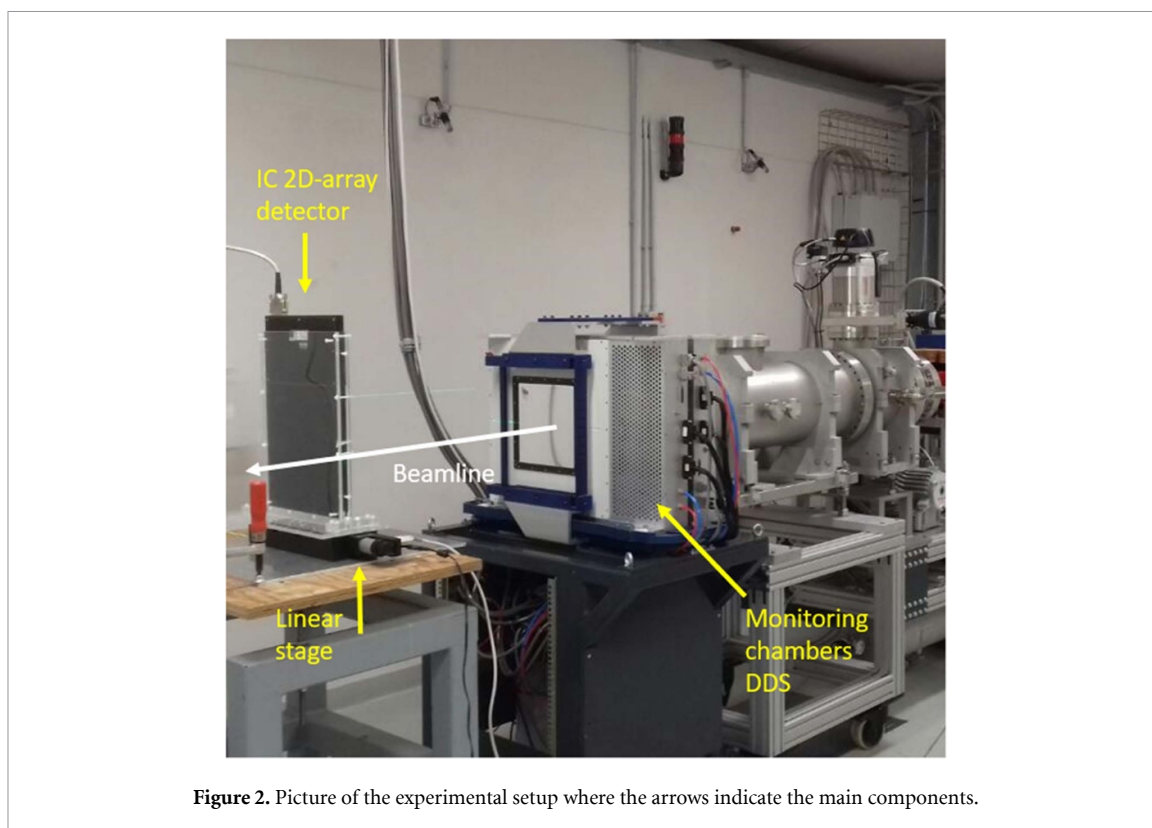


Figure 2. Picture of the experimental setup where the arrows indicate the main components.

publication (Steinsberger *et al* 2021). The periodic motion (4 or 10 phases) was extracted from 25 generated phases covering half of a respiratory cycle between end-exhale and end-inhale phases. For each phase CT, a spherical tumor was placed in the left lung and translated by a constant step per state, covering a total of 40 mm motion amplitude in the CC direction and 10 mm anteroposterior (AP) direction. The end-exhale phase has been chosen as reference CT and all the other frames of the 4DCT are registered to it via Plastimatch.

Three single posterior field plans have been optimized with the treatment planning system TRiP98 (Richter *et al* 2013, Steinsberger *et al* 2021), using a range-ITV (Graeff 2014) and a 4D-optimization strategy called MP4D (Lis *et al* 2020, Steinsberger *et al* 2023). Two plans involve 4 motion phases (target dose of 3 and 5 Gy) and a third plan with 10 phases (target dose of 3 Gy). To simplify the validation process, only absorbed dose was considered. The ITV plan was delivered with and without motion, to evaluate the impact of interplay. These deliveries will be referred to as ‘interplay’ and ‘static’, respectively.

The validation of the algorithm has been divided into four subsections. First, we present the comparison of the developed algorithm for dose distribution warping with Plastimatch. The second section aims at validating the accuracy of the dose reconstruction algorithm. Third, we estimate the time performance of the FDC, and the final section proves the capability of the system to identify delivery errors during treatments.

### 2.3.1. Dose warping benchmark

As mentioned in section 2.3, the algorithm has been updated to handle 4D calculations in real-time, by integrating a very fast algorithm for warping the dose distribution on the reference anatomy. This has been accomplished by porting the standard CPU Plastimatch dose warping algorithm on GPU. To validate the accuracy and test the speed of the system, the warping procedure has been benchmarked against Plastimatch. The CTs of the 10 phases XCAT 4DCT have been generated with 4D-RIDOS and Plastimatch, based on the reference CT and the DVFs out of the Plastimatch registration. The metrics used for defining the accuracy are the median value and the inter-quartile range (IQR) of the absolute difference of voxels intensity in Hounsfield Unit (HU). Besides the accuracy, the processing time of the two algorithms was assessed.

### 2.3.2. Dose calculation accuracy assessment

The dose distributions calculated by 4D-RIDOS have been compared against detector measurements and TRiP98 using log-file based dose reconstructions. The tests conducted in the experimental room at CNAO (section 2.2) cannot be used for assessing the accuracy of the reconstruction. As mentioned in section 2.1.3, 4D-RIDOS requires 3D LUTs with beamline specific quantities to perform the dose calculation, which were

not yet available for the experimental room at CNAO. For this reason, the system has been benchmarked using delivery records and measurements of a previous experimental campaign in a clinical room at CNAO (Steinsberger *et al* 2023). In that study, some of the same plans as the ones described in section 2.3 were delivered: ITV and MP4D plans with 4 and 10 phases. The dose distribution calculated by 4D-RIDOS have been compared against detector measurements and reconstructed doses with TRiP98.

To compare to detector measurements, the doses have been calculated on a homogeneous water cube [200 × 200 × 200, 1 mm<sup>3</sup> voxel size]. The delivered spot positions have been rigidly shifted on the horizontal plane synchronized with the known detector motion, removing the approximation of using discrete motion phases. The agreement was evaluated with a gamma-index analysis with 3%/3 mm criteria.

### 2.3.3. Processing time evaluation

The evaluation of the processing time of the algorithm has been carried out by analyzing the deliveries performed in the experimental room at CNAO.

As explained in section 2.1.3, the end of an energy slice or a change in the motion phase during beam on is taken as a trigger for the dose calculation. In such cases, the GUI sends to the FDC the characteristics of the delivered spots. The operation time has been measured as the timespan between the moment the FDC receives the data and the completion of the dose reconstruction, including dose warping where applicable. Each of these calculations is performed over a given number of spots, depending on the characteristics of the plan and of the delivery. For each delivery modality, the measurements were then averaged over all the tests performed, resulting in a mean reconstruction time per spot. With the same approach, the mean number of spots for each triggered calculation has been calculated.

The time measurements were performed with CUDA built-in functions providing a resolution of 0.5 microseconds, as reported by the official documentation of NVIDIA. It is worth noting that all the reconstructions have been performed considering a constant 17 mm radial cutoff for the calculations.

### 2.3.4. Real-time detection of dose errors

Finally, the tests in the experimental room have been used to provide examples of detecting dose errors in real-time with 4D-RIDOS and 4D-RIDOS expected DVH. Two examples are going to be presented. An interplay delivery reconstructed with 4D-RIDOS showing the impact of motion on a static plan, and an unintentional case of a failure of the power supply of the scanning magnet setting the vertical position while delivering an MP4D (10phases) plan.

## 3. Results

### 3.1. Dose warping benchmark

The warping algorithm quality has been determined by comparing the results against standard Plastimatch running on CPU. The generation of the CTs of the XCAT 4DCT leads to a median value of the difference of 0 HU with an IQR of 0, as expected for implementations of the same algorithms. The average processing time is 66.3 ms (minimum 62.7 ms, std 2.33 ms) for Plastimatch, and it is 3.25 ms (minimum 3.2 ms, std 0.09) for the GPU-based algorithm, respectively.

### 3.2. Dose calculation accuracy assessment

The precision of the dose reconstruction has been validated against detector measurements and TRiP98 log-file calculations, as represented by figure 3.

Figure 3(a) shows the benchmark of 4D-RIDOS against the measured dose of an MP4D delivery with 10 phases. Figures 3(b) and (c), depict the comparison against TRiP98 calculations, in terms of gamma index, for the same delivery reconstructed as a static plan in water, following section 2.3.2. Both TRiP98 and 4D-RIDOS use pencil beam algorithms, but differences in the implementations lead to non-negligible dose differences even for the same base-data, in particular in the distal and lateral margins (figure 3(b)).

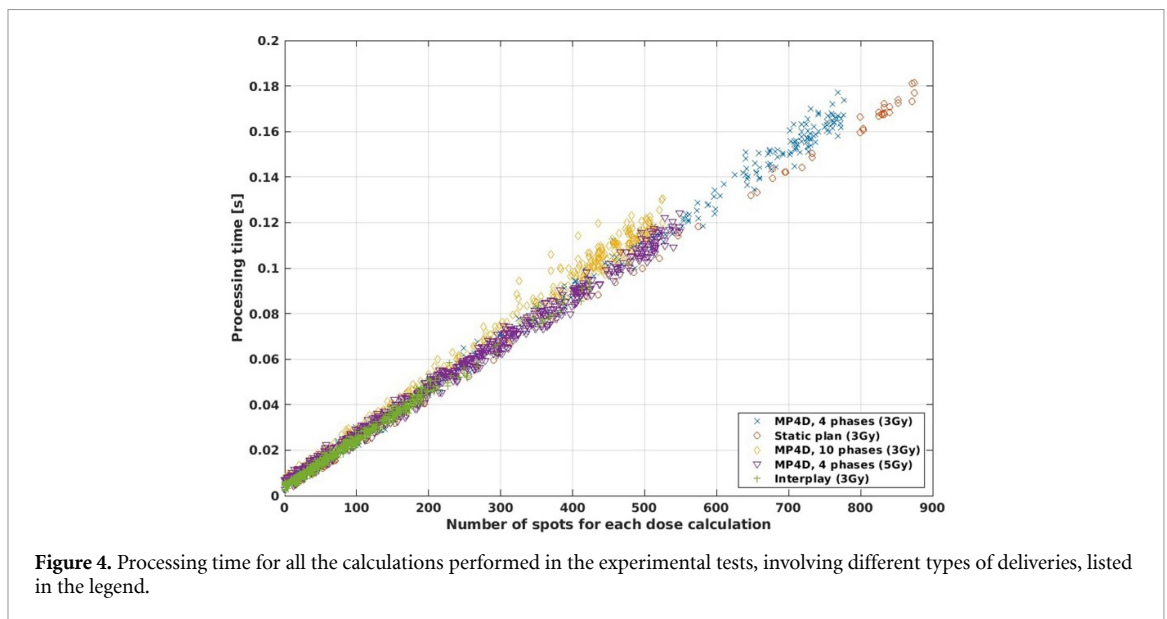
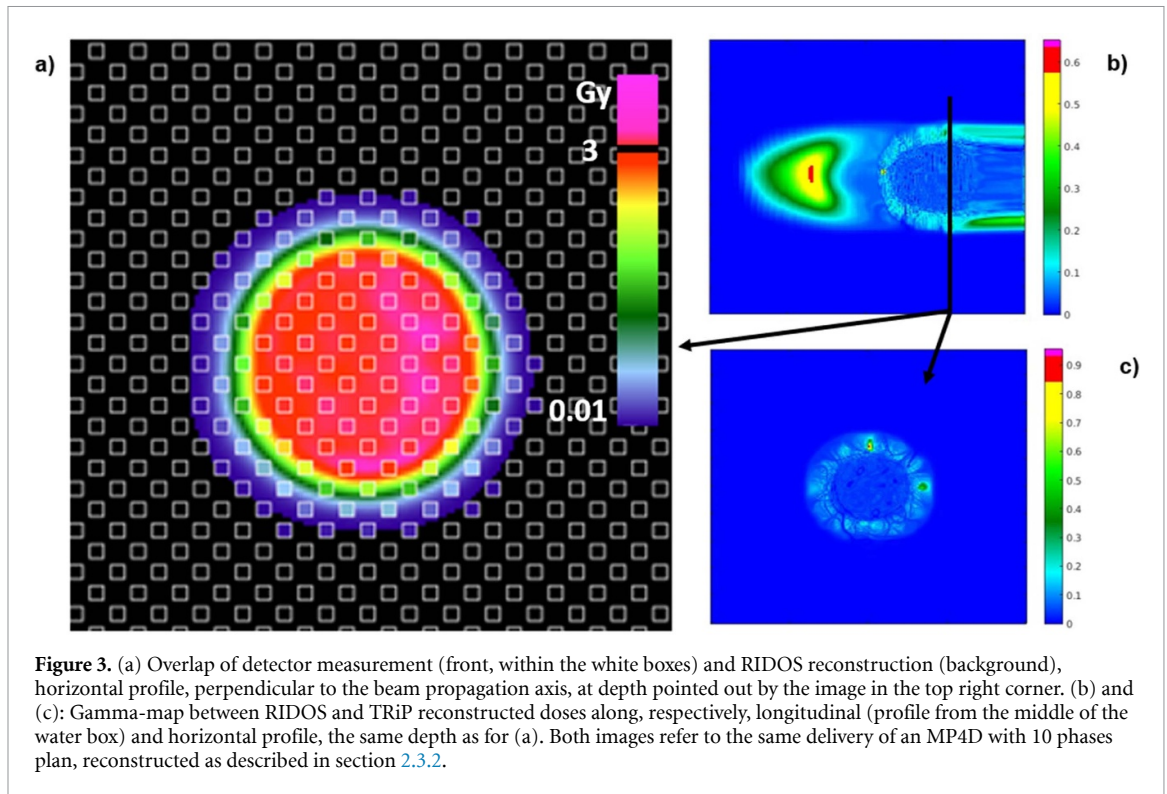
Out of 10 deliveries, the average gamma-index passing rate (3%/3 mm) against detector measurements is 98.3% (min 96.24%, std 1.34%), while against TRiP98 is of 99.78% (min 97.88%, std 0.67%).

### 3.3. Processing time evaluation

The analysis of the processing time has been performed on tests involving five different deliveries: static, interplay, MP4D with 4 phases (3 and 5 Gy) and 10 phases (3 Gy).

An overview of all the processing times collected during the experiments is offered in figure 4. Each point is a calculation with a processing time in seconds on the *y*-axis, and the number of spots on the *x*-axis. The figure shows a proportionality between these two parameters and a globally similar behavior for the different delivery modalities. It is, however, possible to appreciate some differences.





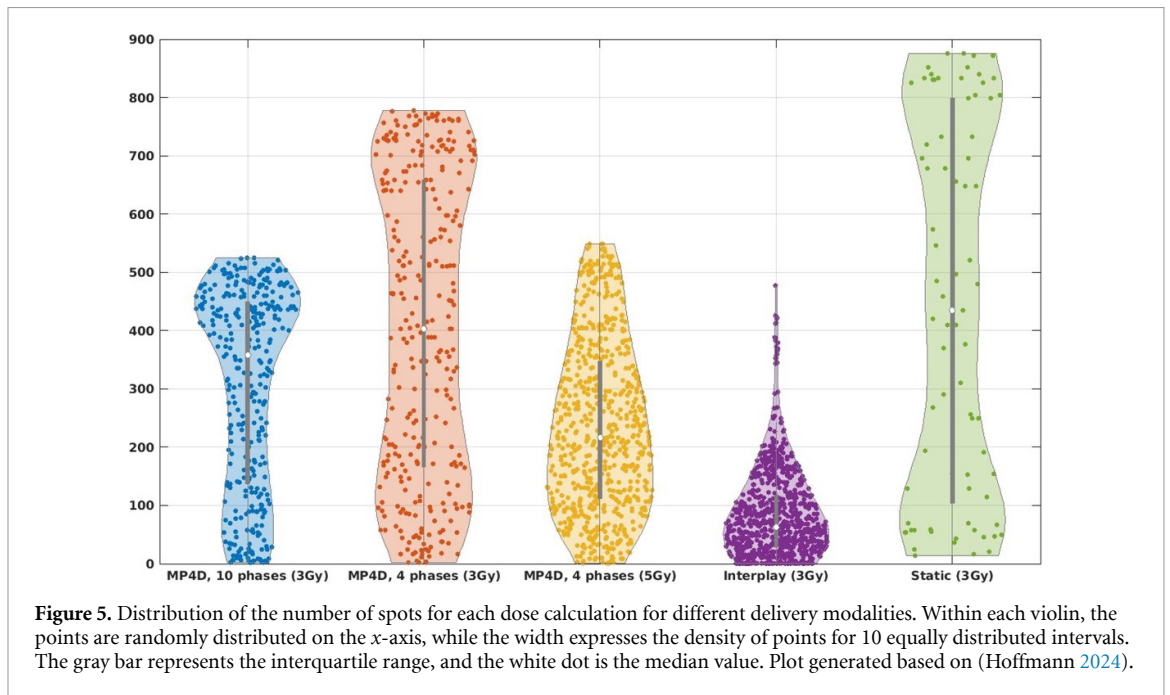
By looking at the processing time for calculations on a consistent number of spots (bigger than 600), is clear that the reconstruction for the static plan is faster than the one for the 4 phases plan with 3 Gy. This can be partially explained by the lack of dose warping (approximately 3 ms) in the static case.

Moreover, the delivery precision proved to be directly connected to the size of the spots due to the limited sensitivity of the beam monitor chambers. In the case of MP4D plans the mean number of particles per spot decreases significantly compared to static or interplay deliveries, putting some pressure on the scanning magnets. This led to several spots delivered not in the planned position, and because of the characteristics of the algorithm, as described in section 2.1.3, the reconstruction of those spots had to be performed on the whole CT, instead of exploiting the precompiled selection of voxels performed prior the delivery. This aspect is made clear in figure 4 by the points representing the 10 phases deliveries, which exhibit a larger processing time compared to the other deliveries.

The mean reconstruction time per spot ranges between 0.22 ms and 0.65 ms (table 1), which corresponds to the deliveries with the highest and the smallest mean number of spots per calculation (static and interplay

**Table 1.** Delivery and dose reconstruction performances for all the tested deliveries.

Plan	Mean delivery time per spot (ms)	Mean reconstruction time per spot (ms)	Mean number of spots per calculation	Mean number of particles per spot (#)
MP4D (10phases, 3 Gy)	0.56	0.38	302	$2.076 \times 10^4$
MP4D (4phases, 3 Gy)	0.80	0.29	402	$3.697 \times 10^4$
MP4D (4phases, 5 Gy)	2.0	0.30	237	$7.300 \times 10^4$
Interplay	2.9	0.65	83	$1.338 \times 10^5$
Static (3 Gy)	2.8	0.22	440	$1.338 \times 10^5$

**Figure 5.** Distribution of the number of spots for each dose calculation for different delivery modalities. Within each violin, the points are randomly distributed on the x-axis, while the width expresses the density of points for 10 equally distributed intervals. The gray bar represents the interquartile range, and the white dot is the median value. Plot generated based on (Hoffmann 2024).

deliveries, respectively). Interplay deliveries show a higher concentration of calculations performed on a small number of spots (figure 5) and this influences the mean processing time per spot, as listed in table 1. Such a relevant difference is connected to the structure of the algorithm. In detail, for each calculation the system allocates the memory and transfers on GPU the LUT required for that specific energy, and accumulates the results over the cumulative planned and delivered dose matrix. These are timely consuming operations, which strongly impact the mean processing time in case of calculations over a small number of spots.

In 4D deliveries, having the change of phase as a trigger to start the reconstruction, it is more common to perform calculations on a smaller number of spots. Moreover, 4D-RIDOS does not compute only on fully delivered spots. It also considers aborted or gated spots in which there is any, despite how small, delivery of particles detected by the monitor chambers, mostly observed at the switch between phases. To distinguish between noise of the monitor chambers and delivery of particles during aborted or gated spots a minimum threshold of 5 Monitor Units, beam monitor output of the charge collected for that spot (Mirandola *et al* 2015), has been set.

As shown in table 1, 4D-RIDOS time performance is mostly influenced by the mean number of spots per calculation. However, the delivery time is always higher than the processing time, and it can be up to more than one order of magnitude larger, like in the case of static plans.

### 3.4. Real-time detection of dose errors

A final section is devoted to the identification of dose errors. The GUI screenshot shown in figure 6 depicts the dose distributions for an interplay delivery, as introduced in section 2.3.4. The severity of the motion on the treatment accuracy is clearly visible by the dose difference box in the bottom-left corner, as well as the percentage of voxels passing the gamma-index analysis slice after slice (slice passing rate box). This is for a 3D-plan delivered to a breathing patient with an extreme motion amplitude, considered in 10 phases. It was chosen here to better highlight the capabilities of 4D-RIDOS for real-time detection of the impact of motion on treatment deliveries.

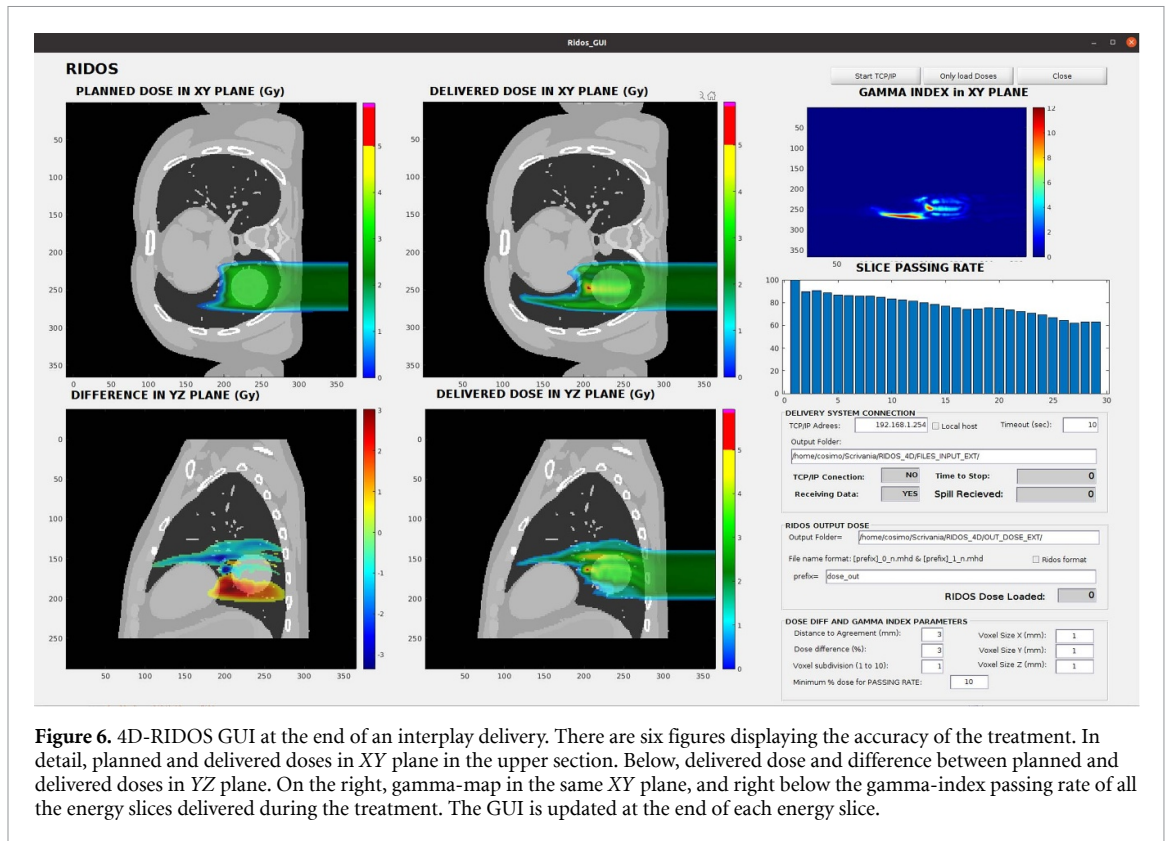


**Figure 6.** 4D-RIDOS GUI at the end of an interplay delivery. There are six figures displaying the accuracy of the treatment. In detail, planned and delivered doses in XY plane in the upper section. Below, delivered dose and difference between planned and delivered doses in YZ plane. On the right, gamma-map in the same XY plane, and right below the gamma-index passing rate of all the energy slices delivered during the treatment. The GUI is updated at the end of each energy slice.

The following image depicts a case happened with an unintentional magnet failure affecting the quality of the treatment (figure 7). As this was an experimental test, the delivery was not stopped but completed as interlocks were masked. The vertical scanning magnet was off for a few slices (from 9 to 12), and then it went back on. This is clear from the slice passing rate box, where at slice 9 the average value dropped from about 100% to 92.86%. The smallest passing rate has been reached after slice 12 with 60.1%. From slice 13 on the magnet started working properly again.

#### 4. Discussion

In this paper we proposed a system named 4D-RIDOS which includes software tools and specific hardware able to perform a 4D real-time dose reconstruction, integrated into the future clinical DDS at CNAO (Lis *et al* 2020, Donetti *et al* 2021, Steinsberger *et al* 2023). The goal is to identify any deviations of the delivered dose from the planned one as soon as possible in a fully automatic fashion, in order to provide this information to the treating physicians and possibly for online or offline adaptation. At the current status, 4D-RIDOS would be able to detect machine errors, like in the case of the failure of the power supply of the magnitude reported in section 3.4, and to provide automatically the reconstruction of the delivered dose at the end of the treatment, or right after the treatment interruption. 4D-RIDOS expected DVH could also be employed to trigger an interrupt of the delivery in case of significant discrepancies between planned and delivered doses. As a visionary challenge, real-time adaptive therapy (Rakita *et al* 2020, Steinsberger *et al* 2023) could exploit the measured dose deviations on the fly. The use of 4D-RIDOS in clinics would limit the burden of the personnel, making available an accurate report of the delivery during the treatment with no further actions required. In addition, 4D-RIDOS can be applied in purely experimental scenarios, to test the efficacy of new motion mitigation strategies at a research stage.

This work represents to our knowledge the first fully integrated 4D real-time dose reconstruction tool developed for particle therapy, following the example of what has been achieved by (Skouboe *et al* 2019) for conventional radiotherapy. Different tools have been developed in the last years for 4D dose reconstructions (Scandurra *et al* 2016, Choi *et al* 2018, Meijers *et al* 2019, Guterres Marmitt *et al* 2020, Duetschler *et al* 2023), but they are all performing the operation retrospectively. Even though this approach would be suitable for online adaptive therapy, a tool such 4D-RIDOS would provide the possibility of adapting in between beams of the same fraction, and it also represents a first step towards real-time adaptation of the plans.

4D-RIDOS was characterized to verify accuracy and speed. The tool has been benchmarked against detector measurements conducted in a clinical room at CNAO with clinically acceptable results, and it proved

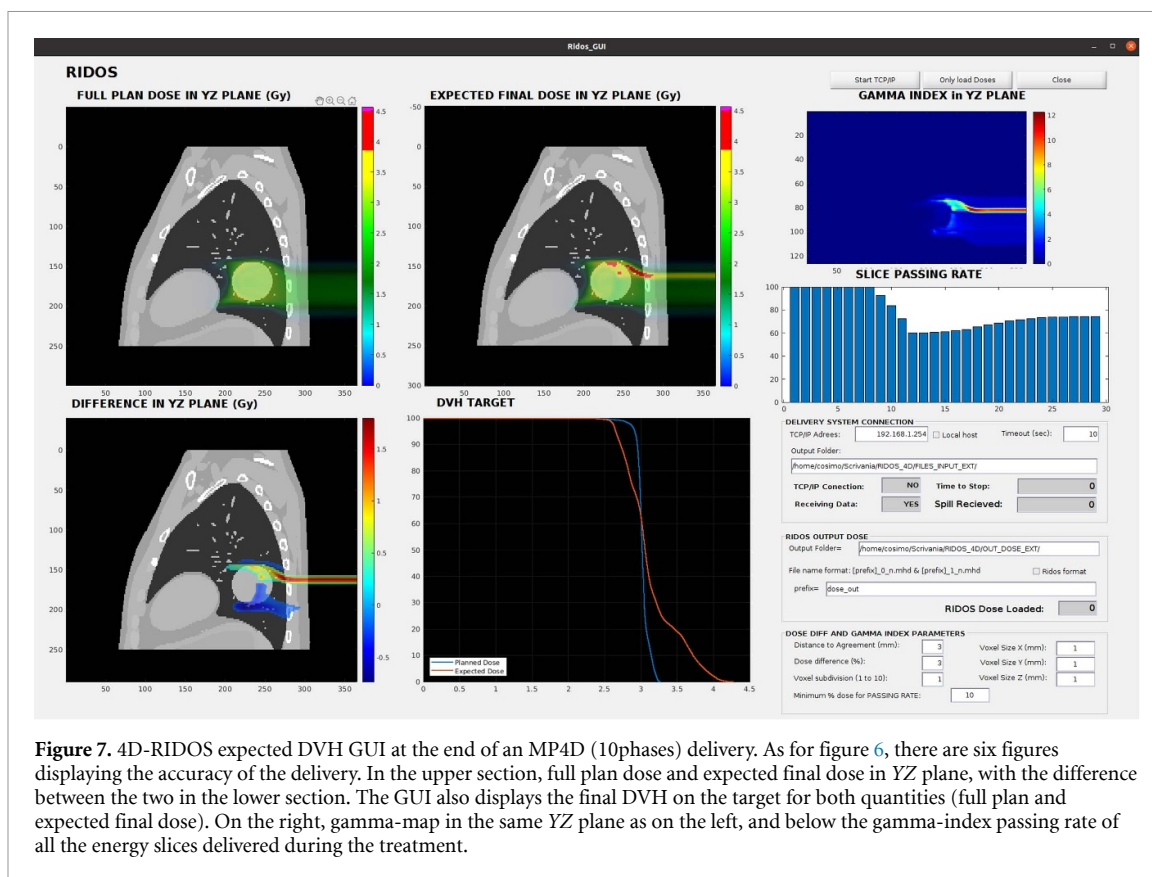


**Figure 7.** 4D-RIDOS expected DVH GUI at the end of an MP4D (10phases) delivery. As for figure 6, there are six figures displaying the accuracy of the delivery. In the upper section, full plan dose and expected final dose in YZ plane, with the difference between the two in the lower section. The GUI also displays the final DVH on the target for both quantities (full plan and expected final dose). On the right, gamma-map in the same YZ plane as on the left, and below the gamma-index passing rate of all the energy slices delivered during the treatment.

to be always faster than the delivery. Moreover, the results were displayed on the GUI and a gamma-index, and DVH analysis in the case of 4D-RIDOS expected DVH, were performed before the start of the delivery of the following energy slice. However, the current implementation of 4D-RIDOS is based on an analytical dose engine, which is subject to inaccuracies, as it cannot represent the true physics of the particles in matter. Monte Carlo dose calculation is widely viewed as the gold standard, but for carbon ion therapy the available Monte Carlo engines are still much too slow for real-time dose calculation (Mein *et al* 2019). Compared to protons, the amount of nuclear interactions and secondary particles that needs to be transported slows down the achievable runtime considerably. While GPU-based Monte Carlo (Schiavi *et al* 2017) are available that are significantly faster than CPU-based simulations, the runtime per pencil beam is in the order of seconds, while for the purpose of this work, runtimes in the order of ms are desired. Recent advances in deep learning dose engines (Neishabouri *et al* 2021, Pastor-Serrano and Perkó 2022) have achieved suitable performance both in terms of speed and accuracy for proton beams, this advance is yet to be translated to carbon ion therapy. The difficulty resides in the prediction of the parameters needed for RBE-weighted dose calculation alongside the dose which can reduce prediction speed and increase uncertainty. Nevertheless, work on a carbon deep learning engine is ongoing and its integration into 4D-RIDOS is planned in the near future.

Despite the dosimetric validation being performed with absorbed dose in water only, 4D-RIDOS includes also the possibility of reconstructing RBE-weighted doses, with an average processing time of 0.45 ms per spot (MP4D plan with 4 phases, 5 Gy) (Galeone *et al* 2023). The algorithm is under further development and testing and the results will be reported in a future publication. The system will also be tested with more complex phantoms, accounting for tissue heterogeneities, which might affect the accuracy of the reconstructed doses. In this context, the introduction of sub-pencils in the dose engine can mitigate some of the inaccuracies related to the analytical dose engine (Yang *et al* 2020), however, the inclusion of deep learning dose prediction models as discussed above will be investigated as well.

One limitation of the current setup was the patient's motion detection. The motion phase was streamed to the DDS by the moving phantom, and it represented the first step towards more realistic clinical scenarios, i.e. the Anzai belt used in (Giordanengo *et al* 2019) or an Optical Tracking System (OTS) (Fattori *et al* 2016). It is worth noting that, the choice of the device detecting and streaming the motion phase will not have any impact on the operation of 4D-RIDOS, but will have an impact on the 4D-dose accuracy. Preliminary tests indicate that motion detection errors in the order of 1–2 mm may already have a considerable impact on the reconstructed doses, which is currently being investigated in more detail.



The current clinical standard, for treatment planning and post hoc dose reconstruction relies on 4DCT, which also sets the basis for real-time dose reconstruction in 4D-RIDOS. 4DCTs have the inherent limitation of representing only a single, averaged, breathing cycle, which is not reflective of the true anatomy during the treatment. Similar, the reconstruction on discrete phases neglects residual errors introduced by the motion of the patient between those breathing phases. For a typical breathing cycle, this motion between phases can be in the order of a few mm, which introduces a non-negligible dose difference if not accounted for. Future expansion of the methods in this work should include continuous representation of the motion by allowing for an interpolation between 4DCT phases, and consider the use of real-time motion guidance information (Fassi *et al* 2015). Different methods to assess the patient's anatomy variations have been published such as x-ray fluoroscopy, real-time MRI (Hoffmann *et al* 2020), and external respiratory surrogates (Fattori *et al* 2016). Current developments in the field of artificial intelligence may provide an interesting option to convert the real-time available motion information into realistic DVFs to the original CT, potentially providing an ideal combination with this work. Still, the above is more likely to cause an underestimation of dosimetric errors, and any differences observed with 4D-RIDOS still indicate a deviation from the original plan. Hence, despite the current limitations, this work presents a promising first step toward real-time dose guided adaptation.

The presented tool was tested with carbon ions but it can work with protons or other ions as well. Switching between particles does not influence the algorithm, which only needs the proper LUTs to be interpolated. However, an increase in the processing time is expected for protons reconstructions because of a larger number of particles per spot leads to an increase in the number of voxels affected by each beam. The increase in the average processing time would be, however, mitigated by the per spot voxels pre-selection algorithm. Moreover, switching between different accelerators would only need an integration with the specific DDS to receive the real-time spot parameters.

The following steps include experiments in a more complex scenario such as anthropomorphic phantoms, for a more exhaustive validation of the algorithm. This represents a crucial point before the ultimate goal of testing the system with real patients.

## 5. Conclusions

The 4D-RIDOS system was shown to be able to perform 4D real-time dose reconstruction at the CNAO research beam line. It has been integrated in the updated version of the clinical dose delivery system capable to manage 4D treatments deliveries.

The system proved to meet the clinical requirements in terms of accuracy and speed, as necessary to achieve the overall goal of identifying the delivered dose errors as soon as possible during the treatment delivery. The 4D-RIDOS system provides prompt feedback on the actual dose delivered, which could be used for plan adaptation and possible interventions, or in research scenarios, to test the efficacy of new motion mitigation strategies. Moreover, our vision is to exploit 4D-RIDOS for mitigating observed dose deviations on the fly in the future.

## Data availability statement

The data cannot be made publicly available upon publication due to legal restrictions preventing unrestricted public distribution. The data that support the findings of this study are available upon reasonable request from the authors.

## Acknowledgments

This study has been funded by the European Union's Horizon 2020 research and innovation program under the Marie Skłodowska-Curie Grant Agreement No. 966956. This work was partially carried on within the SIG\_PNR project of the Istituto Nazionale di Fisica Nucleare under the supervision of the Commissione Scientifica Nazionale 5. The publication is funded by the Open Access Publishing Fund of GSI Helmholtzzentrum fuer Schwerionenforschung.




## ORCID iDs

C Galeone  <https://orcid.org/0009-0006-4048-1728>

M Donetti  <https://orcid.org/0000-0001-7489-6274>

M C Martire  <https://orcid.org/0009-0006-5331-9463>

A Vignati  <https://orcid.org/0000-0001-8137-9080>

L Volz  <https://orcid.org/0000-0003-0441-4350>  
M Durante  <https://orcid.org/0000-0002-4615-553X>  
S Giordanengo  <https://orcid.org/0000-0001-6347-1182>  
C Graeff  <https://orcid.org/0000-0002-5296-7649>

## References

- Albertini F, Matter M, Nenoff L, Zhang Y and Lomax A 2020 Online daily adaptive proton therapy *Br. J. Radiol.* **93** 20190594
- Bertschi S, Stützer K, Berthold J, Pietsch J, Smeets J, Janssens G and Richter C 2023 Potential margin reduction in prostate cancer proton therapy with prompt gamma imaging for online treatment verification *Phys. Imaging Radiat. Oncol.* **26** 100447
- Bobic M, Lalonde A, Sharp G C, Grassberger C, Verburg J M, Winey B A, Lomax A J and Paganetti H 2021 Comparison of weekly and daily online adaptation for head and neck intensity-modulated proton therapy *Phys. Med. Biol.* **66** 055023
- Choi K, Mein S B, Kopp B, Magro G, Molinelli S, Ciocca M and Mairani A 2018 FRoG—a new calculation engine for clinical investigations with proton and carbon ion beams at CNAO *Cancers* **10** 1–14
- Ciocca M et al 2016 Commissioning of the 4-D treatment delivery system for organ motion management in synchrotron-based scanning ion beams *Phys. Med.* **32** 1667–71
- Dhont J et al 2018 The long- and short-term variability of breathing induced tumor motion in lung and liver over the course of a radiotherapy treatment *Radiother. Oncol.* **126** 339–46
- Donetti M et al 2021 Current and future technologies of the CNAO dose delivery system *IEEE Instrum. Meas. Mag.* **24** 61–69
- Duetschler A et al 2023 A motion model-guided 4D dose reconstruction for pencil beam scanned proton therapy A motion model-guided 4D dose reconstruction for pencil beam scanned proton therapy
- Durante M and Loeffler J S 2010 Charged particles in radiation oncology *Nat. Rev. Clin. Oncol.* **7** 37–43
- Fassi A, Seregini M, Riboldi M, Cerveri P, Sarrut D, Ivaldi G B, de Fatis P T, Liotta M and Baroni G 2015 Surrogate-driven deformable motion model for organ motion tracking in particle radiation therapy *Phys. Med. Biol.* **60** 1565–82
- Fattori G et al 2016 Real-time optical tracking for motion compensated irradiation with scanned particle beams at CNAO *Nucl. Inst. Methods Phys. Res. A* **827** 39–45
- Fiorina E et al 2018 Monte Carlo simulation tool for online treatment monitoring in hadrontherapy with in-beam PET: a patient study *Phys. Med.* **51** 71–80
- Galeone C et al 2023 Real-time RBE-weighted 4D-dose calculation for carbon ion therapy *4D Workshop (Villigen, CH)*
- Giordanengo S et al 2015 The CNAO dose delivery system for modulated scanning ion beam radiotherapy *Med. Phys.* **42** 263–75
- Giordanengo S et al 2019 RIDOS: a new system for online computation of the delivered dose distributions in scanning ion beam therapy *Phys. Med.* **60** 139–49
- Graeff C 2014 Motion mitigation in scanned ion beam therapy through 4D-optimization *Phys. Med.* **30** 570–7
- Graeff C et al 2023 Emerging technologies for cancer therapy using accelerated particles *Prog. Part. Nucl. Phys.* **131** 104046
- Grözinger S O, Bert C, Haberer T, Kraft G and Rietzel E 2008 Motion compensation with a scanned ion beam: a technical feasibility study *Radiat. Oncol.* **3** 1–7
- Guterres Marmitt G, Pin A, Ng Wei Siang K, Janssens G, Souris K, Cohilis M, Langendijk J A, Both S, Knopf A and Meijers A 2020 Platform for automatic patient quality assurance via Monte Carlo simulations in proton therapy *Phys. Med.* **70** 49–57
- Hoffmann A et al 2020 MR-guided proton therapy: a review and a preview *Radiat. Oncol.* **15** 1–13
- Hoffmann H 2024 Violin plot *MATLAB Central File Exchange* (available at: [www.mathworks.com/matlabcentral/fileexchange/45134-violin-plot](http://www.mathworks.com/matlabcentral/fileexchange/45134-violin-plot))
- Knopf A-C et al 2022 Clinical necessity of multi-image based (4DMIB) optimization for targets affected by respiratory motion and treated with scanned particle therapy—A comprehensive review *Radiother. Oncol.* **169** 77–85
- Krimmer J, Dauvergne D, Létang J M and Testa É 2018 Prompt-gamma monitoring in hadrontherapy: a review *Nucl. Instrum. Methods Phys. Res. A* **878** 58–73
- Lis M, Donetti M, Newhauser W, Durante M, Dey J, Weber U, Wolf M, Steinsberger T and Graeff C 2020 A modular dose delivery system for treating moving targets with scanned ion beams: performance and safety characteristics, and preliminary tests *Phys. Med.* **76** 307–16
- Lomax A J 2020 Proton therapy special feature: review article myths and realities of range uncertainty *Br. J. Radiol.* **93** 1–9
- Meijers A, Jakobi A, Stützer K, Guterres Marmitt G, Both S, Langendijk J A, Richter C and Knopf A 2019 Log file-based dose reconstruction and accumulation for 4D adaptive pencil beam scanned proton therapy in a clinical treatment planning system: implementation and proof-of-concept *Med. Phys.* **46** 1140–9
- Mein S et al 2019 Dosimetric validation of Monte Carlo and analytical dose engines with raster-scanning 1H, 4He, 12C, and 16O ion-beams using an anthropomorphic phantom *Phys. Med.* **64** 123–31
- Minohara S, Kanai T, Endo M, Noda K and Kanazawa M 2000 Respiratory gated irradiation system for heavy-ion radiotherapy *Int. J. Radiat. Oncol. Biol. Phys.* **47** 1097–103
- Mirandola A et al 2015 Dosimetric commissioning and quality assurance of scanned ion beams at the Italian national center for oncological hadrontherapy *Med. Phys.* **42** 5287–300
- Neishabouri A, Wahl N, Mairani A, Köthe U and Bangert M 2021 Long short-term memory networks for proton dose calculation in highly heterogeneous tissues *Med. Phys.* **48** 1893–908
- Pakela J M et al 2022 Management of motion and anatomical variations in charged particle therapy: past, present, and into the future *Front. Oncol.* **12** 1–16
- Parodi K, Yamaya T and Moskal P 2023 Experience and new prospects of PET imaging for ion beam therapy monitoring *Z. Med. Phys.* **33** 22–34
- Particle Therapy Co-Operative Group 2024 Particle therapy facilities in clinical operation (available at: [www.ptcog.ch/index.php/facilities-in-operation](http://www.ptcog.ch/index.php/facilities-in-operation)) (Accessed 26 April 2024)
- Pastor-Serrano O and Perkó Z 2022 Millisecond speed deep learning based proton dose calculation with Monte Carlo accuracy *Phys. Med. Biol.* **67** 105006
- Persoon L C G G, Podesta M, van Elmpt W J C, Nijsten S M J J G and Verhaegen F 2011 A fast three-dimensional gamma evaluation using a GPU utilizing texture memory for on-the-fly interpolations *Med. Phys.* **38** 4032–5
- Pfeiler T et al 2018 Experimental validation of a 4D dose calculation routine for pencil beam scanning proton therapy *Z. Med. Phys.* **28** 121–33

- Rakita A, Nikolić N, Mildner M, Matiassek J and Elbe-Bürger A 2020 The potential of Gantry beamline large momentum acceptance for real time tumour tracking in pencil beam scanning proton therapy *Sci. Rep.* **10** 1–13
- Riboldi M, Orecchia R and Baroni G 2012 Real-time tumour tracking in particle therapy: technological developments and future perspectives *Lancet Oncol.* **13** e383–91
- Richter D, Schwarzkopf A, Trautmann J, Krämer M, Durante M, Jäkel O and Bert C 2013 Upgrade and benchmarking of a 4D treatment planning system for scanned ion beam therapy *Med. Phys.* **40** 1–17
- Russo G et al 2015 A novel algorithm for the calculation of physical and biological irradiation quantities in scanned ion beam therapy: the beamlet superposition approach *Phys. Med. Biol.* **61** 183–214
- Scandurra D et al 2016 Assessing the quality of proton PBS treatment delivery using machine log files: comprehensive analysis of clinical treatments delivered at PSI Gantry 2 *Phys. Med. Biol.* **61** 1171–81
- Schiavi A, Senzacqua M, Pioli S, Mairani A, Magro G, Molinelli S, Ciocca M, Battistoni G and Patera V 2017 Fred: a GPU-accelerated fast-Monte Carlo code for rapid treatment plan recalculation in ion beam therapy *Phys. Med. Biol.* **62** 7482–504
- Segars W P, Mahesh M, Beck T J, Frey E C and Tsui B M W 2008 Realistic CT simulation using the 4D XCAT phantom *Med. Phys.* **35** 3800–8
- Sharp G et al 2010 Plastimatch: an open source software suite for radiotherapy image processing *Proc. 16th Int. Conf. use Comput. Radiother. (October 2017)*
- Siddon R L 1985 Fast calculation of the exact radiological path for a three-dimensional CT array *Med. Phys.* **12** 252–5
- Skouboe S, Ravkilde T, Bertholet J, Hansen R, Worm E S, Muurholm C G, Weber B, Høyer M and Poulsen P R 2019 First clinical real-time motion-including tumor dose reconstruction during radiotherapy delivery *Radiother. Oncol.* **139** 66–71
- Steinsberger T, Alliger C, Donetti M, Krämer M, Lis M, Paz A, Wolf M and Graeff C 2021 Extension of RBE-weighted 4D particle dose calculation for non-periodic motion *Phys. Med.* **91** 62–72
- Steinsberger T, Donetti M, Lis M, Volz L, Wolf M, Durante M and Graeff C 2023 Experimental validation of a real-time adaptive 4D-optimized particle radiotherapy approach to treat irregularly moving tumors *Int. J. Radiat. Oncol. Biol. Phys.* **115** 1257–68
- The MathWorks Inc. MATLAB 2018b (The MathWorks Inc.)
- Trnkova P et al 2023 A survey of practice patterns for adaptive particle therapy for interfractional changes *Phys. Imaging Radiat. Oncol.* **26** 100442
- Vingelmann P and Fitzek F H P (NVIDIA) CUDA: release 11.6.0 (available at: <https://developer.nvidia.com/cuda-toolkit>)
- Yang J et al 2020 An improved beam splitting method for intensity modulated proton therapy physics in medicine & biology an improved beam splitting method for intensity modulated proton therapy *Phys. Med. Biol.* **65**
- Zhang Y et al 2023 A survey of practice patterns for real-time intrafractional motion-management in particle therapy *Phys. Imaging Radiat. Oncol.* **26** 100439